Load compensation bridge for Josephson arbitrary waveform synthesizers

Frédéric Overney[1] , **Yaowaret Pimsut**[2], **Stephan Bauer**[2] , **Oliver Kieler**[2] ,
Ralf Behr[2] **and Blaise Jeanneret**[1]

[1] Federal Institute of Metrology METAS, Lindenweg 50, CH-3003 Bern-Wabern, Switzerland
[2] Physikalisch-Technische Bundesanstalt PTB, Bundesallee 100, D-38116 Braunschweig, Germany

E-mail: blaise.jeanneret@metas.ch

Abstract
The Josephson arbitrary waveform synthesizer is a quantum-based voltage source that
can generate arbitrary waveforms with quantum accuracy. However, these state-of-the-art
performances are drastically decreased by the wiring connecting the source to the device under
test. This wiring introduces deviations from the Josephson voltage which scale quadratically
with frequency.

This paper describes a load compensation bridge that fully compensates the load of the
Josephson arbitrary waveform synthesizer by the input impedance of the device under test and
completely suppresses the frequency dependence up to a frequency of 80 kHz with an overall
uncertainty of 2.8 µV V^{-1}.

Keywords: impedance comparison, AC Josephson voltage standard, JAWS, digital bridge

(Some figures may appear in colour only in the online journal)

1. Introduction

Josephson arbitrary waveform synthesizers (JAWS) are quantum digital-to-analog converters [1, 2] that produce quantum-accurate and distortion-free voltage waveforms up to frequencies of a MHz. However, the quantum accurate voltage is present at the output of the Josephson junction array inside the cryostat. Twisted-pairs or coaxial cables are bringing this voltage to the input of the device under test (DUT) outside the cryostat. These cables represent a load that causes the voltage, supplied to the DUT, to differ from the Josephson quantized voltage. The voltage leads cause the output voltage to show deviations that quadratically scale with the frequency and with the length of the cables [3]. These frequency-dependent deviations turn out to be the dominant source of uncertainty for frequencies above approximately 10 kHz. Recently, this quadratic frequency dependence was considered in terms of electromagnetic waves reflected by the DUT and the JAWS due to impedance mismatch, even for signal path lengths much

shorter than the signal wavelength [4]. The description of the deviations in terms of reflected waves suggests that solutions can be found in methods commonly used at radio and microwave frequencies to minimize or compensate these reflected waves. The most straightforward solution is using a smaller cryostat to reduce the cable length [5]. However, this length reduction only lowers the deviations by an order of magnitude, it will never fully compensate them. Another method is the detection of the reflected wave using a directional coupler and re-injection of a compensation signal. For wavelengths as long as dealt with in the JAWS setup, this could be achieved using a so-called tandem match coupler, which is used in radio technology [6]. However, this method is known to have a limited accuracy. Another approach is to use impedance matching [6], such that the reflections are minimized. The variation of the voltage measured along the transmission line is minimized when no reflections occur at the source and the load sides. In the method previously described, the influence of the liquid helium level on the cables impedance should be considered carefully, as shown in [7]. Finally, a recent analysis demonstrated how the uncertainties of the transmission line impedance and on-chip inductance impact the accuracy of the rms amplitude conveyed to the DUT [8].
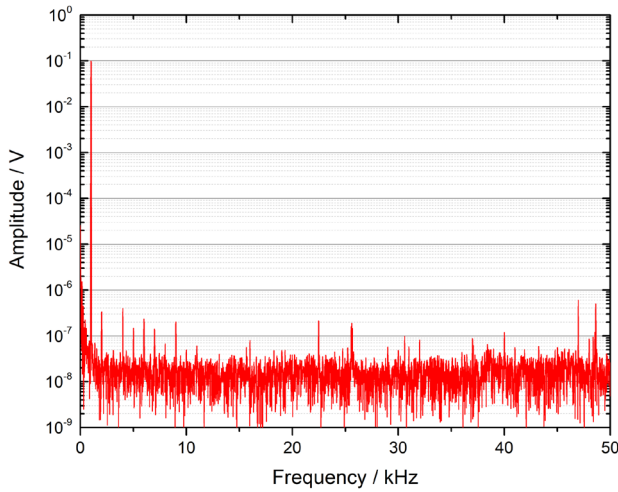
Figure 1. Plot of the measured 1 kHz spectrum obtained at the input of the Fluke 792A while the JAWS system and the LCB were connected. The LCB injection was off (passive). The harmonic components below 10 kHz are attributed to the JAWS system alone (i.e. without the LCB connected). The SFDR for this part of the spectrum is about 108 dB. The other frequency components are attributed to the LCB. The measured SFDR including these components is 104 dB.

Since none of the previous attempts has lead to satisfactory results, a different approach needed to be developed that cancels the loading effect of the cable and decreases the difference between the voltage applied to the DUT and the calculated voltage at the Josephson junction array. This paper presents an original method based on a load compensation bridge (LCB) and shows its practical realisation as well as a set of convincing preliminary results.

2. Josephson arbitrary waveform synthesizer

For the proof of principle experiment, the LCB was combined with a JAWS system based on a pulse driven Josephson array with 12 000 quad-stacked junctions [9]. The array was placed in a liquid helium Dewar using a cryoprobe. The Josephson junctions are driven by pulses provided by a ternary pulse-pattern generator (PPG) which was operated with a clock frequency of around 14 GHz.

The delta-sigma codes used for this LCB setup were of 2nd order, making the measured spurious free dynamic range (SFDR) of the JAWS system itself larger than 108 dB at 1 kHz. This value is comparable to the specification of the measurement device [10]. The quantum locking range (QLR) is the range where the various bias parameters can be changed without a change in the measured spectrum. These QLR were determined with the LCB (passive) and the Fluke 792A connected. The working point of each bias parameter was chosen to be close to the center of the QLR. These values were measured once at the beginning of the measurement period and stored to a settings file. All parameters were regularly checked (see an example in the results section), by determining the QLR of all the bias parameters again. No changes were

observed during the measurement period. Figure 1 shows a spectrum measured at the input of the Fluke 792A at a frequency of at 1 kHz with the complete setup connected.

For this LCB setup the cryoprobe has a triaxial cable and connector for the voltage output. The compensation current for the ac-coupling [11] was delivered by a commercial function generator and a home made electronic source via a 50 Ω coaxial line. One further line was used to connect the reference potential to the Josephson array (see figure 2).

Since the Josephson junctions are arranged within a coplanar waveguide, the array has an intrinsic inductance. This inductance causes a voltage drop of $V_{ind} = 2\pi fIL$. Where f is the signal frequency, I is the compensation current driven trough the array with the inductance L. The measured inductance of the array is about 15 nH. With the needed compensation current I of about 2 mA, this causes an inductive voltage drop at 80 kHz, of about 15 μV over the array. This voltage is in quadrature with the 100 mV Josephson voltage and, therefore, adds quadratically to the voltage measured with the Fluke 792A. The maximum relative error introduced by this inductive voltage is around 1 part in 10^8 and hence negligible for the present measurements.

3. Load compensation bridge

The setup of the load compensation bridge (LCB) is depicted in figure 2 and in the schematic of figure 3 to clarify the bridge's principle. The Josephson voltage, V_{in}, is brought to the DUT by a triaxial cable. The current, i, flowing in the central conductor of this cable, is measured by a 1:100 detection transformer coupled to an ADC (voltage V_i). This current i can be nulled by injecting a current i_s through an impedance Z_s which is biased by a DAC (voltage V_s), feeding a 1:1 double shielded injection transformer. In addition, at the injection point, the first shield of the triax-cable (coloured in blue in figure 2) is connected to the central conductor, forming an active guard, which prevents capacitive current from loading the system [12]. When $i = 0$, the voltage at the DUT, V_{out}, is expected to be equal to the input voltage V_{in}, i.e. the Josephson voltage.

At this point, a couple of important comments must be made:

- The distance between the reference planes (dotted lines in figure 2) for the voltages V_{out}, V_{in} and the detection point—where i is measured- has to be identical.
- The requirements on the stability and noise of the voltage V_s is mitigated by a factor Z_c/Z_s, in which Z_c is the impedance of the connecting cable of the JAWS. This factor can be made as small as 10^{-4} by choosing a high value for Z_s (see [13] for a detailed description).
- When the bridge is balanced, no current flows through the central conductor of the cable. Therefore, a variation of its impedance, due to a variation of the He-level, will have a negligible effect on the voltage V_{out} applied to the DUT.
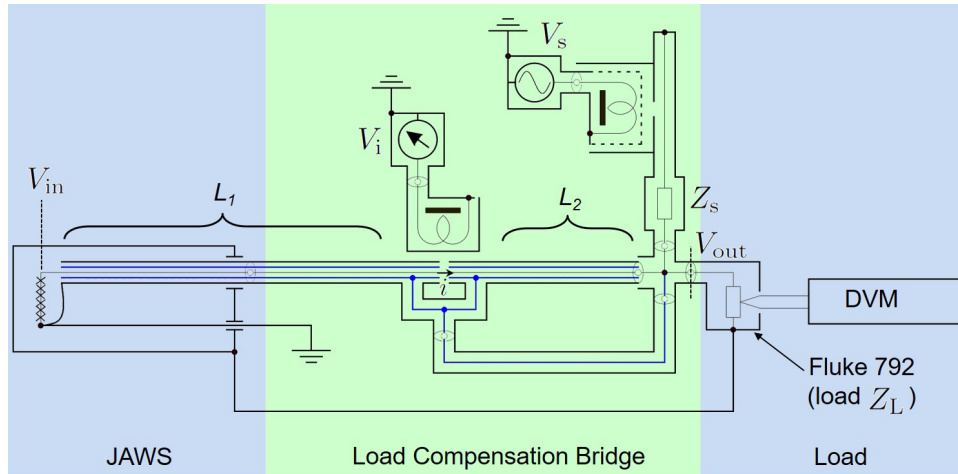
Figure 2. Schematic of the load compensation bridge. The input voltage, V_{in}, is the JAWS voltage which is connected to the bridge using a triaxial cable. At the injection point, an external current i_s is injected through Z_s in the central conductor of the triaxial cable using a DAC voltage V_s (see figure 3). At the very same point the first shield of the triaxial cable (coloured in blue) is connected to the central conductor, forming an active guard which prevents capacitive currents to flow to ground. The bridge is balanced by tuning V_s until the current i flowing in the central connector is zero. This current is sensed by a detection transformer coupled to a low noise ADC (voltage V_i). The output voltage, V_{out}, is read by a Fluke 792A thermal transfer standard of impedance Z_L.

The hardware components like the detection and injection transformers are home made. The DACs and ADCs are National Instrument multi-purpose boards type NI PXI 4461 which limit the maximum frequency to 80 kHz.

To connect the LCB to the Josephson junction array, the cryoprobe had to be custom wired with triaxial wiring. The length of this wire (L_1 in figure 2) had to be determined precisely to match the length of the LCB cables (length L_2 in figure 2), according to the comment above. For this specific setup the length L_1 and L_2 were matched to within ±5 mm. The mechanical matching of the wiring will ensure that the electrical length (i.e. the length determining the impedance of the line) of both side of the wiring will be as close as possible.

The output voltage of the LCB is read by a freshly calibrated Fluke 792A thermal transfer standard coupled to a digital multimeter (Keysight 3458A).

The software controlling the LCB-running on the master computer-is able to balance the bridge fully automatically for a given set of frequencies and voltages making overnight measurement possible. The full automation requires that the LCB software also control the JAWS software-running on a slave computer—to select any required voltage and frequency. This was achieved using a LabVIEW TCP protocol. Finally, the LCB software also reads the output voltage of the Fluke 792A through the multimeter.

Both the JAWS sytsem and the LCB bridge are synchronized on the same 10 MHz clock [14] to allow coherent sampling of V_i and coherent generation of V_S. Moreover, the data processing and the balance procedure are fully described in [15].

4. Results

The measurements carried out were based on ac–ac differences performed at constant amplitude. The reference frequency was chosen to be 1 kHz, a frequency at which the
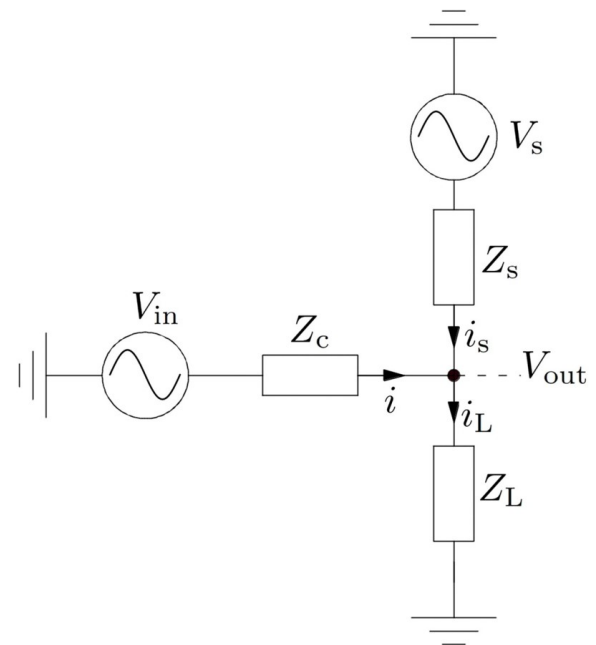

Figure 3. Equivalent circuit of the load compensation bridge depicted in figure 2.

effect of capacitive loading is known to be much smaller than 1 μV V^{-1}. After every high-frequency measurement, a control measurement at 1 kHz was performed to take the drift of the instruments into account. The relative difference $\Delta V / V_{1\ kHz} = (V - V_{1\ kHz}) / V_{1\ kHz}$ between the control measurement and the high-frequency result is reported in the graphics.

The effect of the LCB is demonstrated in figure 4. The quadratic frequency dependence observed when the LCB is not active is in agreement with previous measurements with similar systems [4, 6, 16]. Deviations as large as a few hundred of μV V^{-1} are observed at 80 kHz. Once balanced the LCB has a dramatic effect on the measurements i.e. the quadratic
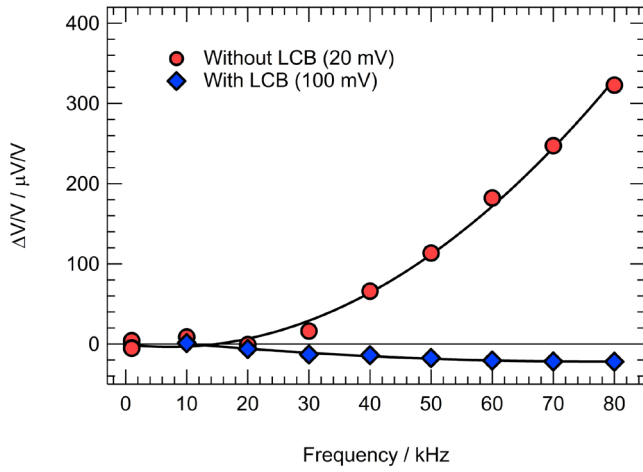
Figure 4. Voltage measured at the output of the Fluke 792, expressed as the relative difference to 1 kHz, as a function of the frequency. The red curve was measured at 20 mV without injecting any compensation current with the LCB. A clear quadratic frequency dependence is observed. The blue curve was measured at 100 mV after the LCB is fully balanced. The frequency dependence is strongly attenuated up to 80 kHz.
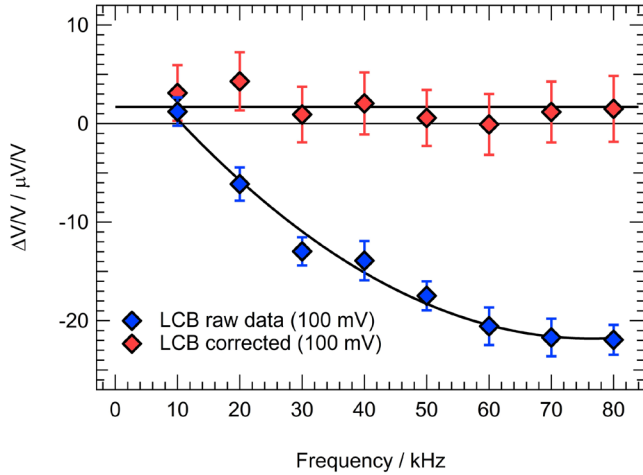

Figure 5. In blue: The data at 100 mV from figure 4 are plotted in an enlarged scale. In red: Data corrected with the fresh calibration of the Fluke 792A thermal transfer standard. The impact of the LCB is clearly visible: the frequency dependence has been completely suppressed within the measurement uncertainties. The uncertainty bars are for a coverage factor of $k = 1$.

background is severely suppressed. To gain further insight in the LCB performances the data at 100 mV are plotted alone in an enlarged scale in figure 5. At that scale the raw data (blue diamonds in figure 5) still reveal a non-negligible frequency dependence. The uncertainty bars on the data points are 1.7 μV V^{-1} (Type A uncertainty with $k = 1$).

However, these data must be corrected with the calibration values of the Fluke 792A thermal transfer standard. The corrected data are plotted as red diamonds in figure 5. The final result is striking: the frequency dependence has been completely suppressed within the measurement uncertainties demonstrating the effectiveness of the LCB. The corrected data averaged to 1.7 μV V^{-1} with a standard deviation of
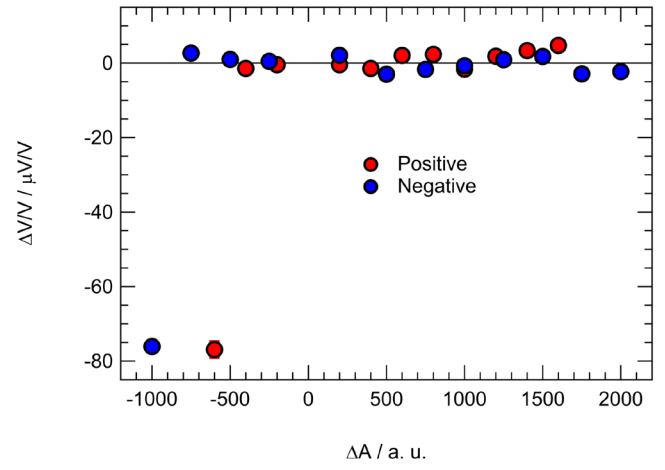
Figure 6. Measurement of the quantum locking range of the JAWS at 80 kHz expressed as a function the amplitude difference ΔA between the actual value of the amplitude and the amplitude at the working point. The graphs demonstrate that the output voltage of the Josephson junction array is independent of the pulse amplitude (both positive and negative) over a broad range. The upper reachable pulse amplitudes is limited by the max output power of the pulse pattern generator (PPG). This limitation does not allow the observation of the high side of the quantum locking range.
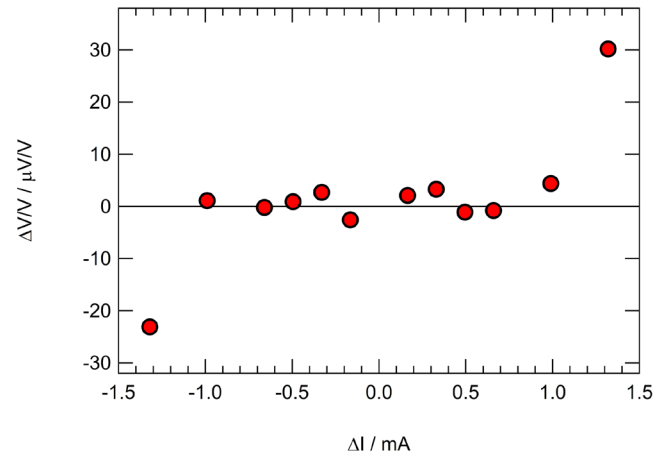
Figure 7. Quantum locking range measurements at 80 kHz expressed as a function of the compensation current difference ΔI between the actual value and the compensation current at the working point. As expected, no dependence on the compensation current is observed over a range of 2 mA.

1.4 μV V^{-1}. This standard deviation is smaller than the uncertainty of the individual data points which is 2.8 μV V^{-1}. For these corrected data, the type A uncertainty had to be combined with the calibration uncertainty of the Fluke 792A (in the 220 mV range) which is the dominant factor.

For the full determination of the uncertainty budget, two additional effects will have to be evaluated:

- The length of the cable injecting the current in the central conductor will produce a change in the phase of the current injected in the bridge.
- The influence of the length difference ($\Delta L = L_1 - L_2$) between the triaxial cables connecting the JJA and the bridge will affect the equilibrium of the bridge.

Finally, the quantum locking range of the JAWS must be periodically checked during the course of the measurements to ensure that the pulse driven array (JJA) really works as a quantum standard. The output voltage of the JJA must be independent of any of its bias parameters over a certain range. An example of the measurement of the quantum locking range is shown in figures 6 and 7, where the output voltage is shown to be independent of the pulse amplitude (both positive and negative) and of the compensation current, thus providing confidence in the appropriate functioning of the JAWS.

5. Conclusion

This paper has shown that the original approach undertaken in this work by implementing a load compensation bridge is extremely successful. Using an active guard to compensate the capacitive current drawn by the system wiring, the quadratic frequency dependence present at the output terminal of the JAWS was completely eliminated within the measurement uncertainties. Presently, the uncertainty of the load compensation bridge is limited by the calibration of the DUT and amounts to 2.8 μV V^{-1} for a voltage of 100 mV and frequencies up to 80 kHz ($k = 1$). The influence of several additional parameters must be studied in details to expend its working range (both in frequency and voltage) and to further reduce its uncertainty. This paper must be considered as a first preliminary attempt that will certainly be completed by additional systematic studies in the near future.

ORCID iDs

Frédéric Overney https://orcid.org/0000-0002-6845-3132
Stephan Bauer https://orcid.org/0000-0001-6242-2223
Oliver Kieler https://orcid.org/0000-0001-5193-8910
Ralf Behr https://orcid.org/0000-0002-5480-443X

Blaise Jeanneret https://orcid.org/0000-0003-1113-5253

References

[1] Benz S P *et al* 2015 Performance improvements for the NIST 1 V Josephson arbitrary waveform synthesizer *IEEE Trans. Appl. Supercond.* **25** 1400105

[2] Flowers-Jacobs N E, Fox A E, Dresselhaus P D, Schwall R E and Benz S P 2016 Two-volt Josephson arbitrary waveform synthesizer using Wilkinson dividers *IEEE Trans. Appl. Supercond.* **26** 1400207

[3] Filipski P S, Boecker M, Benz S P and Burroughs C J 2011 Experimental determination of the voltage lead error in an ac Josephson voltage standard *IEEE Trans. Instrum. Meas.* **60** 2387–92

[4] van den Brom H E, Zhao D and Houtzager E 2016 Voltage lead errors in an AC Josephson voltage standard: explanation in terms of standing waves *2016 Conf. on Precision Electromagnetic Measurements* (IEEE) pp 1–2

[5] van den Brom H E, Kieler O F, Bauer S and Houtzager E 2017 AC–DC calibrations with a pulse-driven AC Josephson Voltage standard operated in a small cryostat *IEEE Trans. Instrum. Meas.* **66** 1391–6

[6] Zhao D, van den Brom H E and Houtzager E 2017 Mitigating voltage lead errors of an AC Josephson voltage standard by impedance matching *Meas. Sci. Technol.* **28** 095004

[7] Kinard J R and Lipe T E 2012 Influence of liquid helium level on dip probe wiring *2012 Conf. on Precision electromagnetic Measurements* (IEEE) pp 546–7

[8] Underwood J M 2019 Uncertainty analysis for ac–dc difference measurements with the AC Josephson voltage standard *Metrologia* **56** 015012

[9] Kieler O *et al* 2015 Towards a 1 V Josephson arbitrary waveform synthesizer *IEEE Trans. Appl. Supercond.* **25** pp 1–5

[10] NI PXI-5922 specifications 2019 www.ni.com/pdf/manuals/374033b.pdf (accessed: 23 October 2019)

[11] Benz S P, Burroughs C J and Dresselhaus P D 2001 Ac coupling technique for Josephson waveform synthesis *IEEE Trans. Appl. Supercond.* **11** 612–6

[12] Hanke R 1989 An improved straddling method with triaxial guards for the calibration of inductive voltage dividers at 1592 Hz *IEEE Trans. Instrum. Meas.* **38** 974–8

[13] Overney F *et al* 2016 Josephson-based full digital bridge for high-accuracy impedance comparisons *Metrologia* **53** 1045–53

[14] Overney F and Mortara A 2014 Synchronization of sampling-based measuring systesm *IEEE Trans. Instrum. Meas.* **63** 89–95

[15] Overney F, Lüönd F and Jeanneret B 2016 Broadband fully automated digitally assisted coaxial bridge for high accuracy impedance ratio measurements *Metrologia* **53** 918–26

[16] van den Brom H E and Houtzager E 2012 Voltage lead corrections for a pulse-driven ac Josephson voltage standard *Meas. Sci. Technol.* **23** 124007